Transition from *Normal* to *Fast* Sound in Liquid Water

F. Sette,[1] G. Ruocco,[2] M. Krisch,[1] C. Masciovecchio,[1] R. Verbeni,[1] and U. Bergmann[1]
[1]*European Synchrotron Radiation Facility, B.P. 220, F-38043 Grenoble, Cedex France*
[2]*Universitá di L'Aquila and Istituto Nazionale di Fisica della Materia, I-67100, L'Aquila, Italy*
(Received 1 April 1996)

Inelastic x-ray scattering data from water at 5 °C show a variation of the velocity of sound from 2000 to 3200 m/s in the momentum transfer range $1-4\ \mathrm{nm}^{-1}$. The transition occurs when, at ≈4 meV, the energy of the sound excitations equals that of a second weakly dispersing mode. This mode is reminiscent of a phonon branch in ice I*h* crystals, which is shown here to be of optical transverse character. The present work accounts for most of the highly debated difference between hydrodynamic (≈1500 m/s) and high-frequency (≈3200 m/s) velocities of sound in water. [S0031-9007(96)00500-5]

PACS numbers: 61.10.Eq, 63.50.+x, 78.70.Ck

Water, in its liquid and solid forms, continues to fascinate for its complicated and quite unique properties. An interesting and still highly debated issue is the phenomenon of *fast* sound in the liquid. The velocity of acousticlike excitations, which is ≈1500 m/s in the hydrodynamic limit up to momentum transfers $Q \approx 2 \times 10^{-2}\ \mathrm{nm}^{-1}$, reaches the value of ≈3200 m/s (fast sound) at Q above $4\ \mathrm{nm}^{-1}$. This large velocity increase was first predicted in a molecular dynamics (MD) calculation [1], which generated a great number of MD simulations aiming to understand the microscopic origin of this process [2,3]. The fast sound was first shown to exist using coherent inelastic neutron scattering (INS) [4]. Recently, it was confirmed in a wider Q region using inelastic x-ray scattering (IXS) [5], and, still using IXS, it was found that the velocity of sound is equivalent in liquid and solid (ice I*h*) water in the whole investigated $4-14\ \mathrm{nm}^{-1}$ Q region [6]. These results confirm the existence of fast sound, show that at high frequencies the dynamical response of the liquid becomes solidlike, and imply that in the liquid the processes responsible for the large variation in the speed of sound must take place in the mesoscopic (Q-ω) region with Q in the $\approx 0.05-4\ \mathrm{nm}^{-1}$ range. This region, too high for light scattering, is also experimentally difficult to reach for both INS and IXS techniques.

In this Letter we report IXS data on water and ice I*h*. The data on water were taken down to a Q transfer of $1\ \mathrm{nm}^{-1}$ using ≈21.75 keV x rays with 1.4 meV energy resolution. They show that the velocity of sound of the longitudinal acousticlike dynamics goes from 2000 m/s at $Q = 1\ \mathrm{nm}^{-1}$ to the fast sound value of 3200 m/s at $Q \geq 4\ \mathrm{nm}^{-1}$. This transition is observed when the longitudinal acoustic dispersion crosses a second branch, observed at ≈4 meV at Q larger than $4\ \mathrm{nm}^{-1}$, and no longer visible at Q smaller than $2\ \mathrm{nm}^{-1}$. We also report IXS data on ice I*h* crystals where we identify at 5–7 meV a transverse optical phonon branch. We suggest that the mode at ≈4 meV in water is reminiscent of this transverse dynamics in ice, although its observation in the present experiment implies that it does not have a pure transverse symmetry as in the crystal. Consequently, we propose that it is the coupling between the acousticlike and opticlike dynamics that gives rise to at least most of the change from normal to fast sound.

The experiment was carried out at the very high energy resolution inelastic x-ray scattering beam line (BL21-ID16) at the European Synchrotron Radiation Facility. The undulator x-ray source was monochromatized using a Si(111) double crystal monochromator and a high energy resolution backscattering monochromator [7], operating either at the Si(999) or at the (11 11 11) Bragg reflections. The scattered photons were collected by a grooved spherical silicon crystal analyzer operating also at the same Bragg backreflections, and in Rowland geometry [8]. The total energy resolution function was measured from the elastic scattering of a plastic sample at its maximum in the static structure factor. The energy resolutions were 3.2 and 1.4 meV full width at half maximum (FWHM) at the Si(999) and (11 11 11) reflections, respectively. The scattering angle for momentum transfers between 2 and $21\ \mathrm{nm}^{-1}$ was selected by rotating the 7 m analyzer arm in the horizontal scattering plane. The Q resolution was set by an aperture in front of the analyzer. Energy scans were done by varying the relative temperature between the monochromator and analyzer crystals. Further experimental details are given elsewhere [5,7,8]. The water sample was high purity H_2O kept at 5 °C in the liquid measurements and at −10 °C in the solid. The solid samples were in the I*h* crystal structure. The dispersion was measured in a polycrystal, and in a single crystal along the (10-11) crystallographic direction. The ice samples were grown *in situ* following established procedures [9]. The samples' thicknesses were ≈18 mm in the direction of the incident beam.

Inelastic x-ray scattering spectra from liquid water at 5 °C, taken with 1.4 meV energy resolution, are shown in Fig. 1 at selected Q together with the results of the

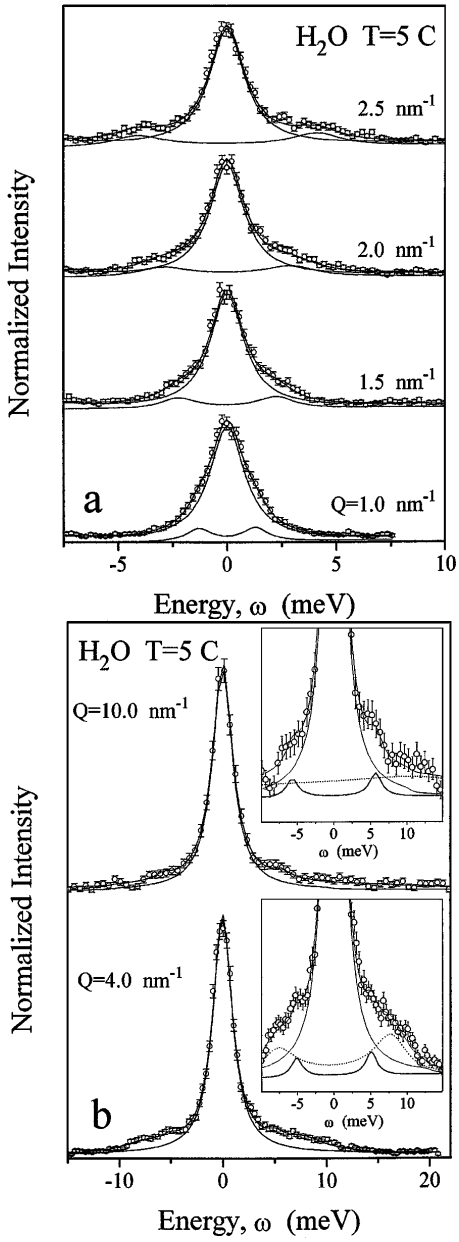

FIG. 1. The IXS spectra of water at $T = 5\,^{\circ}\mathrm{C}$ ($\circ$) shown together with the total fits and the individual components, as explained in the text, at the indicated Q values. The data are normalized to their maximum intensity corresponding to (a) 1.4, 1.2, 1.1, 1.0 counts/s and total counts of 450, 360, 360, 350 at $Q = 1.0, 1.5, 2.0, 2.5\ \mathrm{nm}^{-1}$, respectively; (b) 2.8 and 2.4 counts/s (total counts 1100 and 500) at $Q = 4$ and $10\ \mathrm{nm}^{-1}$, respectively. The insets of (b) emphasize the weakly dispersing features at $\approx$4–5 meV together with the total fit and the individual components. The Q resolution was 0.2 and $0.4\ \mathrm{nm}^{-1}$ for the data in (a) and (b), respectively.

fits discussed in the following. In Fig. 1(a) we report the data taken at the lowest investigated Q values. The data are normalized to the maximum of the central peak. At the sides of the quasielastic central line, with a width of 1.0 ± 0.5 meV FWHM, it is possible to observe inelastic scattered intensity at energies changing with Q. The data have been fitted with a model function consisting of a Lorentzian for the central line and a damped harmonic oscillator (DHO) [10] for the two side bands. The detailed balance has been imposed. The DHO model was used to derive the spectroscopic parameters $\Omega(Q)$ and $\Gamma(Q)$, as defined in [5], independently of specific theories, and to compare them with previous studies also using the same model [4–6]. The fitting function is the convolution of the model with the experimentally determined resolution function. The fit was based on χ^2 minimization, and the results were always within its standard deviation. Similarly, in Fig. 1(b), we show examples of data taken at higher Q values. Beside the inelastic scattered intensity dispersing with Q and already observed in [4,5], thanks to the increased energy resolution it is now possible to observe a new weakly dispersing feature with 4–6 meV energy transfer. This is emphasized in the insets of Fig. 1(b). This feature is observed only in the spectra with Q larger than $4\ \mathrm{nm}^{-1}$, and is no longer detected in the spectra at small Q. This observation is consistent with previous neutron data taken at Q values between 6 and $25\ \mathrm{nm}^{-1}$, where the same excitation was found at 4–6 meV [11,12]. Similar to the data in Fig. 1(a), the data at $Q \geq 4\ \mathrm{nm}^{-1}$ were fitted by a Lorentzian for the central peak and a DHO model for each of the two (dispersing and weakly dispersing) features.

The energies of the excitations, determined from the fit and corresponding to the DHO fitting parameter $\Omega(Q)$, are reported in Fig. 2. The data taken in the present experiment are shown together with those determined by IXS with 3.2 meV [6] and 5 meV [5] energy resolutions. The different measurements of the dispersing excitations are consistent among each other in the common Q range, and correspond to a sound velocity of $v_\infty = 3200\ \mathrm{m/s}$ (dotted line in Fig. 2). This branch is due to the acousticlike modes propagating at these Q values with a sound velocity equivalent to that of the solid [6]. The values of the widths are also consistent among each other, and are reported elsewhere [13]. At Q smaller than $4\ \mathrm{nm}^{-1}$, as emphasized in the inset of Fig. 2, $\Omega(Q)$ no longer follows the dispersion with slope v_∞, and shows a bend down towards the hydrodynamic dispersion law with slope $v_0 \approx 1500\ \mathrm{m/s}$. In Fig. 2 are also reported the peak positions of the weakly dispersing excitations. It is important to notice that the bend down of the acoustic branch takes place when the energy of the acoustic mode equals the one of the weakly dispersing feature. This observation, together with the disappearance of the excitation at 4 meV at Q smaller than $2\ \mathrm{nm}^{-1}$, strongly supports the idea that the transition from the fast sound toward the normal sound is triggered by the degeneracy between these two modes, observed at $Q \approx 4\,\mathrm{nm}^{-1}$.

The Q dependence of the sound velocity, $v(Q) = \Omega(Q)/Q$, derived from the data of Fig. 2, is reported in

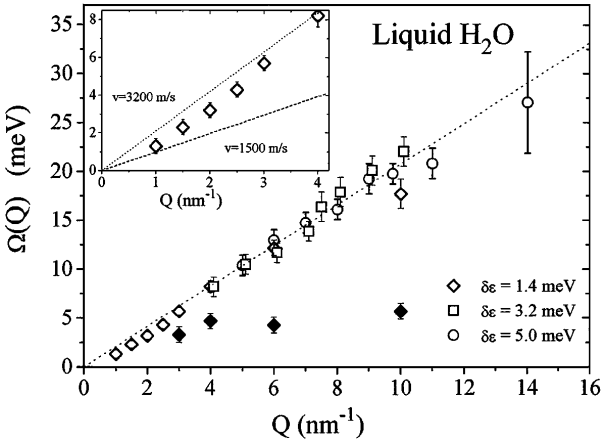

FIG. 2. Excitation energies, $\Omega(Q)$ from the DHO model, for the new high resolution data ($\diamond$, $\delta\epsilon = 1.4$ meV) and from previous IXS experiments ($\square$, $\delta\epsilon = 3.2$ meV [6]; $\circ$, $\delta\epsilon = 5.0$ meV, [5]). The open symbols refer to the dispersing excitation and the full diamond to the weakly dispersing ones. The dotted line, with a slope of 3200 m/s results from a fit for $Q \geq 4$ nm^{-1}. The inset shows an enlargement of the low Q region, where the transition from fast toward normal sound takes place, as emphasized by the two lines corresponding to the fast and normal sound branches.

Fig. 3 together with INS data [4] and MD simulations data [2,3]. The speed of sound decreases from v_∞ to 2000 m/s at $Q = 1$ nm^{-1}. This reduction is well reproduced by the MD calculation of Sciortino and Sastry [3], although at Q larger than 6 nm^{-1} the agreement is much less satisfactory. In this region the potential model used by Balucani *et al.* [2] shows a better consistency.

A possible relation between the dispersion of the longitudinal dynamics and the feature at 4–5 meV was first pointed out by Sastry, Sciortino, and Stanley in a MD calculation performed at Q values larger than 3.3 nm^{-1}

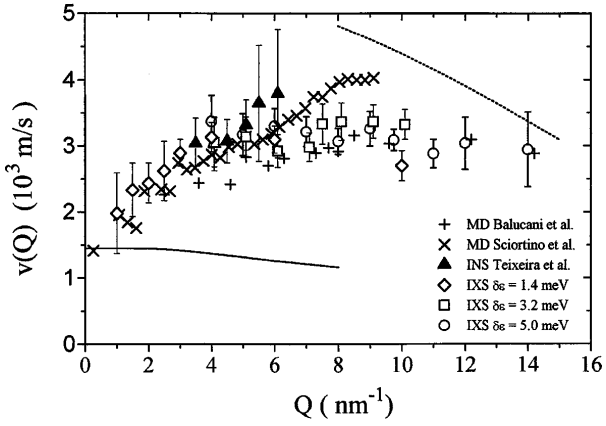

FIG. 3. Values of the sound velocity $v(Q) = \Omega(Q)/Q$ determined from the present ($\diamond$), previous IXS ($\square$ [6], $\circ$ [5]), previous INS data (full $\triangle$), and MD simulations ($+$ [2], $\times$ [3]). The full and dashed line represent the infinite- and zero-frequency limit as derived in Ref. [2].

[14]. These authors derived the mode dispersing with fast sound, as well as a second one with very small dispersion at $\approx$4–6 meV. This last mode was associated to the O-O-O bending. In view of the strong similarities in the longitudinal dynamics of liquid and solid water [6], a study of the ice crystal can shed further information on the nature of the weakly dispersing feature, and on its role in the transition from normal to fast sound.

In Fig. 4 we report IXS data of the $S(Q, \omega)$ for an ice polycrystal at selected Q values and the corresponding fits. Data taken along the (10-11) direction in an ice single crystal are almost identical to those of Fig. 4. The measurements were performed at -10 °C, with 3.2 meV energy resolution. At low Q the spectra are dominated by a feature dispersing with Q, which is identified with the longitudinal acoustic phonon branch, LA [6,15]. The

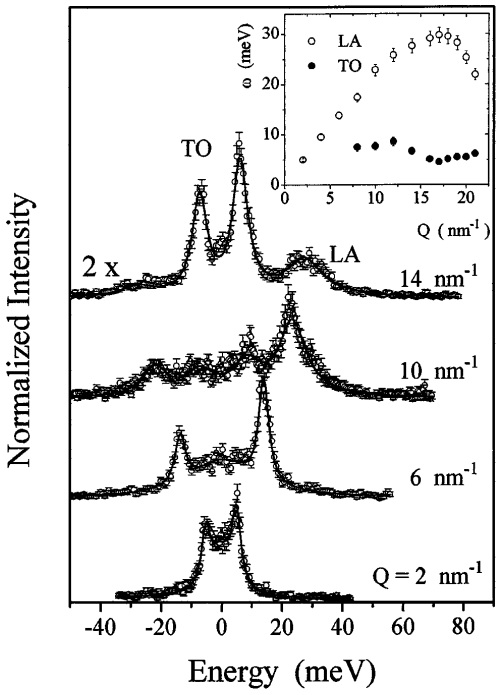

FIG. 4. The IXS spectra of polycrystalline H_2O ice Ih at -10 °C, taken at the indicated Q values with 3.2 meV and 0.4 nm^{-1} energy and momentum resolutions, are reported together with their fits. The longitudinal acoustic and the transverse optical phonons are labeled with LA and TO, respectively. The experimental data are normalized to the maximum of the LA Stokes peak. On this point, the count rates were $\approx$1 count/s at all the investigated Q values. The integration time for each data point was 180 s at $Q = 2$ and 6 nm^{-1} and 90 s at $Q = 10$ and 14 nm^{-1}. The data ($\circ$), shown with the error bars, are superimposed to the fit (solid line). The fit was made by the convolution of the experimental resolution function with two pairs of Lorentzians representing the LA and TO Stokes and anti-Stokes peaks. A fifth Lorentzian was used to account for the small elastic intensity probably due to residual disorder in the polycrystal. In the inset we report the dispersion relation for the LA and TO branches. The speed of sound of the LA branch is 3200 m/s. Note that the TO peak can be observed only at Q larger than 7 nm^{-1}.

dispersion of the LA phonons is shown in the inset of Fig. 4. The peak at $\approx 5-7$ meV, labeled TO, appears only at Q larger than ≈ 7 nm^{-1}, sharply increases in intensity with increasing Q, and dominates the spectrum at Q larger than 10 nm^{-1}. The Q value of ≈ 7.5 nm^{-1} corresponds to the smallest size of the reduced Brillouin zone in ice. Therefore, the intensity behavior of the TO mode indicates that this branch has a very strong transverse symmetry through the whole Brillouin zone [16]. Moreover, the weak dispersion of the TO peaks, as seen in the inset of Fig. 4, allows us to identify them as the lowest transverse optic phonon branch. This assignment is consistent with lattice dynamics calculations [15], but disagrees with the proposed interpretation of neutron data taken in the second and higher Brillouin zones [12]. These neutron data extend in energy only up to the TO peaks and are fully consistent with the present IXS data. The TO branch, however, was interpreted as the ice longitudinal acoustic branch [12]. This confusion, which also contributed to the erroneous assignment of the mode observed at a similar energy in water to the high Q limit of the normal sound excitations in the liquid [11,12], is now removed by the strong polarization dependence of the mode reported here.

The transverse optical character of the branch observed in ice at $5-7$ meV suggests that the feature observed in water at approximately the same energy has the same origin, i.e., is reminiscent of a transverse optical dynamics. The absence of translational invariance in the liquid, however, does not allow modes with pure symmetry. Therefore, differently from ice where the two modes cannot mix, in liquid water they can interact as soon as their energies become comparable. This interaction is likely to be responsible for the determination of two regions with distinctively different longitudinal dynamics: (i) a region including the hydrodynamic regime with a longitudinal dynamics characterized by the normal sound and (ii) a high Q region with a longitudinal-like and transverselike dynamics very similar to those of the solid. The transition between the two regions takes place when the excitation energies of the longitudinal-like propagating dynamics becomes comparable to that of the transverselike dynamics with its much more localized nature.

In conclusion, thanks to the extension of the accessible Q region down to 1 nm^{-1}, it has been possible to demonstrate experimentally that the fast sound branch arises from a bend-up of the normal sound, and that this process takes place at the crossing of the acoustic branch with an opticlike dynamics. These findings account for almost the whole difference between v_∞ and v_0. The difference between the lowest value measured here of ≈ 2000 m/s and v_0 can be due either to the present limit in reaching lower Q values or to the presence of other relaxation processes as suggested in a recent Brillouin light scattering experiment [17]. Further investigations on the possible temperature dependence of the Q value characterizing the transition may resolve this issue.

We acknowledge B. Gorges, for his technical assistance, and U. Balucani and M. Sampoli for useful discussion.

[1] A. Rahman and F. H. Stllinger, Phys. Rev. A **10**, 368 (1974).
[2] U. Balucani, G. Ruocco, A. Torcini, and R. Vallauri, Phys. Rev. E **47**, 1677 (1993).
[3] F. Sciortino and S. Sastry, J. Chem. Phys. **100**, 3881 (1994).
[4] J. Teixeira, M. C. Bellissant-Funel, S. H. Chen, and B. Dorner, Phys. Rev. Lett. **54**, 2681 (1985).
[5] F. Sette, G. Ruocco, M. Krisch, U. Bergmann, C. Masciovecchio, V. Mazzacurati, G. Signorelli, and R. Verbeni, Phys. Rev. Lett. **75**, 850 (1995).
[6] G. Ruocco, F. Sette, U. Bergmann, M. Krisch, C. Masciovecchio, V. Mazzacurati, G. Signorelli, and R. Verbeni, Nature (London) **379**, 521 (1996).
[7] R. Verbeni, F. Sette, M. Krisch, U. Bergmann, B. Gorges, C. Halcoussis, K. Martel, C. Masciovecchio, J. F. Ribois, G. Ruocco, and H. Sinn, J. Synch. Rad. **3**, 62 (1996).
[8] C. Masciovecchio, U. Bergmann, M. Krisch, G. Ruocco, F. Sette, and R. Verbeni, Nucl. Inst. Methods **B111**, 181 (1996).
[9] P. V. Hobbs, *Ice Physics* (Clarendon Press, Oxford, 1974).
[10] B. Fak and B. Dorner, Institute Laue Langevin, Grenoble, France, Report No. 92FA008S, 1992 (unpublished).
[11] P. Bosi, F. Dupre', F. Menzinger, F. Sacchetti, and M. C. Spinelli, Nuovo Cimento Lett. **21**, 436 (1978).
[12] F. J. Bermejo, M. Alvarez, S. M. Bennington, and R. Vallauri, Phys. Rev. E **51**, 2250 (1995).
[13] F. Sette, G. Ruocco, M. Krisch, U. Bergmann, C. Masciovecchio, V. Mazzacurati, G. Signorelli, and R. Verbeni, Phys. Rev. Lett. **76**, 3657 (1996).
[14] S. Sastry, F. Sciortino, and H. E. Stanley, J. Chem. Phys. **95**, 7775 (1991).
[15] P. Bosi, R. Tubino, and G. Zerbi, J. Chem. Phys. **59**, 4578 (1973).
[16] This is due to the selection rules in the one-phonon approximation, which allows one to detect in first Brillouin zone only longitudinal modes, while transverse modes can be detected in higher zones.
[17] A. Cunsolo and M. Nardone (to be published).